



Power Grid Analysis Technologies Contributing to Wind Power Expansion

Koki HAMASAKI*, Takumi IIMURA, Kazuhiro KURODA,
Tetsuya ADACHI, Norihisa NAGASAKI, and Hiroyuki UEMURA

Wind power generation is being increasingly adopted as a renewable energy source. Especially in large-scale wind farm (WF) systems, turbine sites are often located far from substations. When long AC cables are installed, the risk of abnormal phenomena occurrence increases due to the cable capacitance. This paper introduces the interactions between iron-core equipment, such as transformers, used in the WF system, and cable capacitance. Furthermore, this paper shows the contribution of simulations in advance by power grid analysis technologies to realize stable operation of the WF system. The paper also presents the results of experiments validating abnormal phenomena, using a small transformer.

Keywords: wind farm, long-distance cable, grid analysis, current zero-missing phenomenon, magnetizing inrush current

1. Introduction

The Seventh Strategic Energy Plan, adopted by a cabinet decision in February 2025, defines that the renewable energy in total power generation is expected to increase from about 20% in 2022 to 40 or 50% by 2040.⁽¹⁾ In Japan, while photovoltaic power generation has been introduced as the main renewable energy source, wind power generation, particularly wind farm (WF) systems, has also attracted attention because there are many promising areas and upcoming areas.⁽²⁾

However, concerns have been raised about the risk of decreased electricity quality by introducing a large amount of renewable energy. Because there have been few large-scale WF projects, it is difficult to perform verification to avoid the risk due to lack of operational data. Grid analysis technologies, which aim to conduct simulation analyses based on the grid conditions, identify issues, and study possible measures, will play an increasingly important role.

Our grid analysis technologies have an advantage underpinned by a proven track record in elucidating circuit phenomena related to reactive power compensation equipment and power quality management equipment, such as harmonic filters and power capacitors. By leveraging these technologies, we predict potential abnormal phenomena, which may occur on electrical circuits, in advance and propose appropriate system configurations (including equipment layout and capacity) and operating methods, thereby contributing to safe and stable system operation.

This paper explains grid analysis for large-scale WF systems. Chapter 2 describes the characteristics of the required analysis for grid connection of large-scale WFs. Chapter 3 details analyses that should be conducted on a current zero-missing phenomenon, which represents abnormal phenomena that emerge when grid connection cables are long. Chapter 4 explains transformer magnetizing inrush current, one of the important factors in the preliminary evaluation and study for stable operation of WF systems. Chapter 5 introduces the verification results of the circuit phenomena, which are explained in Chapters 3 and 4, using a small transformer for verification.

2. Characteristics of Grid Analysis of WF Systems

In recent years, there has been a growing number of large-scale 100 MW-class WFs. Many technical studies are required until operation commences. Key examples include analyses on abnormal phenomena, preliminary evaluations of stable system operation (Fig. 1), and evaluations of effectiveness and performance based on equipment fabrication and on-site verification. These studies can be conducted by using grid analysis technologies.

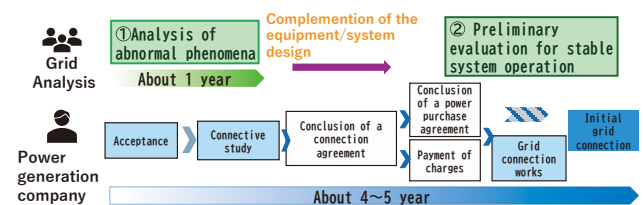


Fig. 1. Process required until the grid of a wind farm (WF) system is connected

Figure 2 shows an example of a large-capacity onshore WF system. Because large-capacity onshore WFs are installed at sites with favorable wind conditions, long distances are common to an existing power transmission line or the grid connection point of a power company

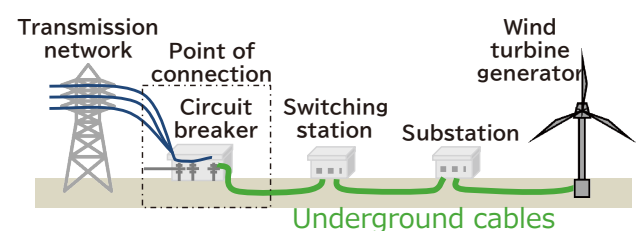


Fig. 2. Example of a WF system

substation. For this reason, wind power generation companies often construct private lines from wind turbines to grid connection points. In construction projects, underground power transmission and long-distance alternating current (AC) cables are used because of less site constraints and shorter construction periods compared to overhead power transmission. However, this has posed technical issues peculiar to long-distance AC cables.

As described above, WFs are constructed in areas with favorable wind conditions. Thus, multiple WFs are likely to be connected to the same power grid bus bar. For this reason, it will become necessary to take into account the effect of other nearby WF systems, in addition to the effect of individual WF systems. Furthermore, these issues will likely become more complex for offshore WFs, which are expected to expand in the future.

Our group offers comprehensive solutions⁽³⁾ covering cables and substation equipment. We have been working to elucidate the mechanisms of these issues and propose measures by harnessing our proprietary grid analysis technologies.

3. Analysis of Abnormal Phenomena of Large-Scale WF Systems

Figure 3 presents an example of main equipment configuration, with the WF system in Fig. 2 illustrated as an electrical circuit. The power grid and a wind turbine generator are connected via a power transmission cable, and the cable's leading reactive power is compensated. Thus, a shunt reactor (ShR) for the positive-sequence and a neutral point grounding ShR (NGL) for the zero sequence are installed in the grid connection switching station. A harmonic filter is installed as a measure against harmonic resonance, and the filter's leading reactive power, which is produced as a byproduct, is compensated by the ShR.

The structure of a crosslinked-polyethylene-insulated vinyl sheath (CV) cable, which is used for power transmission from WFs, is shown in Fig. 4. The cable is formed by multiple concentric layers. It mainly consists of a conductor, through which current flows, an insulator, which electrically insulates the conductor and prevents current from flowing outside the conductor, and a metallic sheath (shielding layer), which prevents the electric field generated by the conductor from leaking outside. In this structure, two electrodes, namely, the conductor and the metallic sheath, are arranged facing each other. When voltage is applied to the cable, positive and negative electric charges

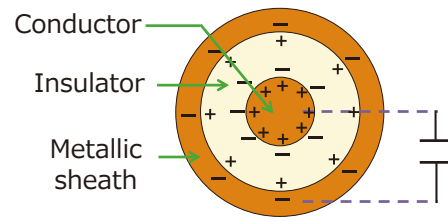


Fig. 4. Cable structure

accumulate in the respective electrodes. Accordingly, a power cable functions as a capacitor from the viewpoint of the power grid.

Table 1 shows abnormal phenomena caused by grid connection via long-distance cables. When a newly built WF is connected to the power grid, the power generation company must conduct a study and implement measures so that the WF will not affect the upstream grid. When we analyze abnormal phenomena by utilizing our grid technologies, we study the items in Table 1 and propose equipment and operation to cope with such phenomena if it is necessary to implement measures.

Table 1. Abnormal phenomena which occur during grid connection via long-distance cables

Phenomenon	Effect
Harmonic resonance ⁽⁴⁾	<ul style="list-style-type: none"> Overheating/noise in customer equipment Overcurrent (due to resonance)
Voltage rise due to cable capacitance	<ul style="list-style-type: none"> Violation of voltage regulation limits by a power company for the grid connection bus bar Insulation deterioration due to exceeding the cable breakdown voltage
Current zero-missing phenomenon (Section 3-1)	<ul style="list-style-type: none"> Interruption failure due to insufficient current-zero duration Wear of circuit breaker terminals
Residual voltage in cable	<ul style="list-style-type: none"> Damage to equipment by closing a circuit breaker when residual voltage is present

3-1 Study of short-circuit current zero-missing phenomenon

This section explains a short-circuit current zero-missing phenomenon, which represents abnormal phenomena listed in Table 1, at which the circuit breaker (CB) tripping is blocked when a short-circuit fault occurs in the grid connection bus bar, and its simulation.

When a reactor, such as a ShR and NGL, is installed in a circuit, transient direct current (DC) is superimposed on the reactor current depending on the timing of a fault or reactor energization. When the cable charging capacity is compensated by a reactor, as in the case of WFs, the above-mentioned DC flows through the grid connection CB and prevents the current from crossing zero. This is likely to block the CB tripping. This is known as a current zero-missing.⁽⁵⁾

This study evaluates whether the grid connection CB can be tripped in the event of a short-circuit fault (i.e., whether current crosses zero). It should be noted that, with respect to the study on current zero-missing, the severe condition in which a wind turbine stops, namely, when

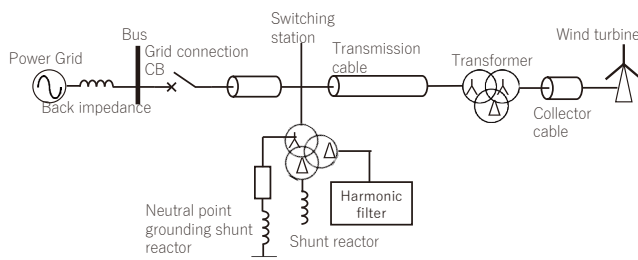


Fig. 3. Example of a WF system circuit

current generated by the wind turbine generator does not flow to the grid connection point, is often studied.

(1) Working principle

The conceptual image of a short-circuit current zero missing phenomenon is shown in Fig. 5. When a short-circuit fault occurs at the grid connection point, the energy stored in the cable compensation ShR is discharged as decaying DC to the fault point, as indicated by the waveform in the middle panel of Fig. 5.

When a wind turbine stops, the WF is isolated from the grid side due to a short-circuit fault. Thus, no AC is supplied from the wind turbine or the grid. Only the transient oscillating current generated by the release of the electric charge from the cable, along with the current with a DC component from the ShR, flows through the grid connection point CB. This results in a period when the current does not cross zero.

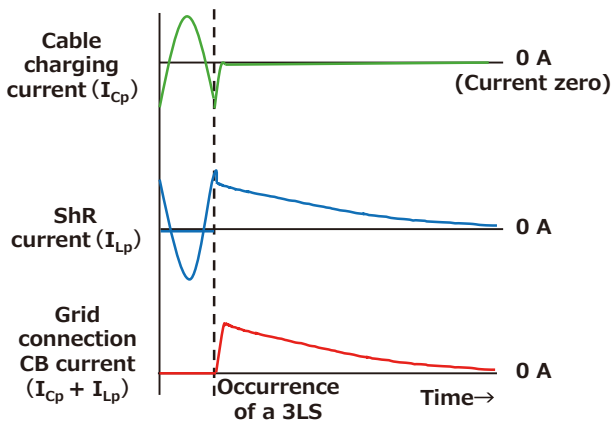


Fig. 5. State of current in the event of a short-circuit current zero-missing

(2) Analysis example

An electrical circuit is simulated in the transient phenomenon analysis software using system configuration diagrams and equipment parameters on the grid/WF premises. A short-circuit fault is triggered on the grid connection bus bar, and the time until current flowing through the grid connection CB crosses zero is confirmed.

As an analysis example, Fig. 6 shows transformer primary-side current at a grid connection switching station that incorporates a ShR and current flowing through the grid connection CB in the event of a three-phase short circuit (3LS) on a grid connection bus bar in the circuit configuration indicated in Fig. 3. As explained in the section of the working principle, the figure shows that the energy stored in the ShR flows to the fault point as current with a DC component, whose decay time is determined by the inductance components and resistance components between the ShR and the fault point.

In this analysis example, transient oscillating components generated by the release of cable electric charges are superimposed on current flowing through grid connection CB, in addition to current with a DC component.

Regarding current zero-missing, including short-circuit current zero-missing, transient oscillating current signifi-

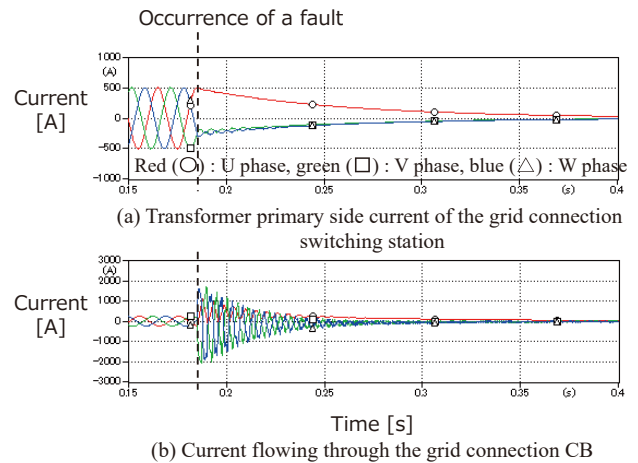


Fig. 6. Simulation results of a short-circuit current zero crossing

cantly affects the time when current flowing through the grid connection CB crosses zero. The oscillating current profile varies depending on the inductance and capacitance elements on the circuit. Circuit phenomena that occur on operational grids can be predicted by harnessing our expertise in actual circuits.

4. Preliminary Evaluation for Stable System Operation

To ensure stable operation when introducing a new system, such as a large-scale WF system, it is necessary to conduct a study both in normal operation and under special circumstances. Table 2 shows examples of study items for stable system operation. One of them is the evaluation of the effect of overvoltage/overcurrent which occurs when starting equipment or in the event of a voltage dip and power restoration. Here, the state of overvoltage/overcurrent by factoring in non-linear characteristics on the circuit, which is difficult to evaluate based on steady-state calculations alone, is evaluated using transient phenomena simulation.

Table 2. Examples studied for a preliminary evaluation to ensure stable system

Item	Evaluation point
Overvoltage/overcurrent when starting equipment	<ul style="list-style-type: none"> Effect on the insulation withstand capability of equipment Effect on the relay operation of the CB due to magnetizing inrush current (Section 4-1), oscillating current, and lightning
Overvoltage/overcurrent in the event of a voltage dip/power restoration	
Lightning on a steel tower (when there is an overhead section)	

4-1 Effect of magnetizing inrush current generated when voltage is applied

This section focuses on magnetizing inrush current, one of the factors that contribute to overcurrent when starting equipment or in the event of a voltage dip and

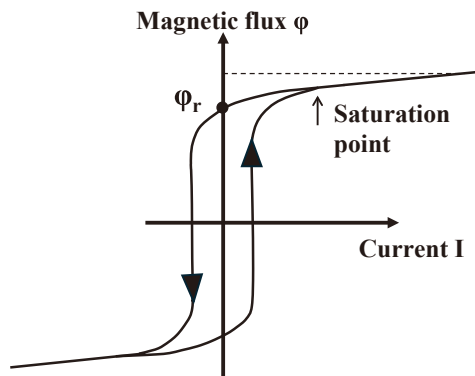
power restoration. It refers to transient current which flows when voltage is applied to a transformer and is up to about 10-fold that of the rated current of a transformer. The points for evaluating the effect of magnetizing inrush current when connecting a WF to the grid are as follows.

- Effect on the overcurrent withstand capability of equipment
- Effect of overcurrent on protection relays
- Expansion of inrush current to power factor correction capacitors / harmonic filters

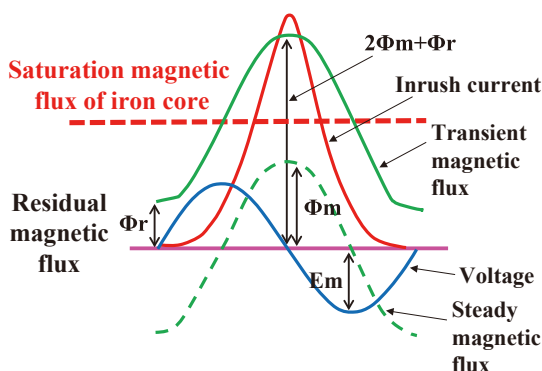
(1) Working principle

Figure 7 shows the mechanism of magnetizing inrush current. Residual magnetic flux ϕ_r is a magnetic flux that remains in the iron core after transformer interruption. In the event of interruption at current zero, the magnetic flux of ϕ_r in Fig. 7 (a) is the residual magnetic flux. Given that the magnetic flux is calculated by integration of voltage, when a transformer is energized at the zero-voltage point, the magnitude of the magnetic flux is maximized (twice the rated current). Here, the residual magnetic flux is also added, causing the magnetic flux to exceed the saturation point of the iron core and resulting in a sharp increase in current. As shown in Fig. 7 (b), twice the magnetic flux plus the residual magnetic flux is the maximum value of the magnetic flux.

In the case of high voltage transformers that we focus on, magnetizing inrush current is likely to continue for several seconds in a low-resistance grid.



(a) Hysteresis loop (I-φ characteristics)



(b) Conceptual diagram of magnetizing inrush current

Fig. 7. Mechanism of magnetizing inrush current

(2) Analysis example

As in the case of the study of current zero missing, the effect of magnetizing inrush current is evaluated using a simulated circuit using the circuit software. Figure 8 shows current which flows through the CB on the transformer primary side when the grid connection switching station transformer in Fig. 3 is energized. The simulation results are used to evaluate whether magnetizing inrush current remains within the withstand capability of equipment or may affect the protection relay.

Potential measures against magnetizing inrush current include the use of phase control and resistors, such as inrush current suppressors. It is also necessary to take precautions against the following phenomena involving magnetizing inrush current.

- Effect of flux contribution from the Δ connection of a transformer (Section 5-2)
- Magnetizing inrush current components flowing into the L = 6% capacitor installed near a WF

Our expertise in circuit phenomena as a transformer and reactor manufacturer enables preliminary verification based on high-precision simulation.

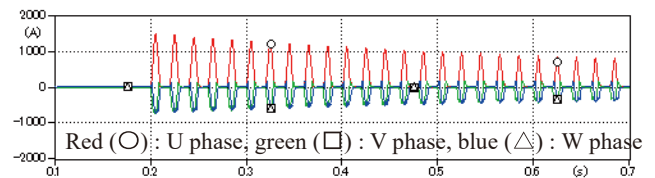


Fig. 8. Current flowing through the CB on the primary side when the grid connection switching station transformer is energized

5. Verification Using a Small-Scale Model of a Transformer

As described above, WF systems are large-scale in general. Thus, simulation must be used to conduct various types of analyses. Instantaneous-value analysis software is widely used for analyses around the world, and the circuit calculation techniques have been well established. However, it is also important to conduct comparative studies based on actual measurement using small-scale models. Notably, transformers are characterized by a simple configuration comprising iron cores and windings. However, it is difficult to perform a full simulation because of non-linearity, in which characteristics change due to saturation of the iron core. For this reason, we develop small-scale models so that we can evaluate the study items related to iron-core equipment based on actual measurement.

Regarding verification using small-scale models, we present two examples used to evaluate short-circuit current zero crossing (3-1) and magnetizing inrush current (4-1).

5-1 Evaluation test of short-circuit current zero-missing phenomenon

Figure 9 shows a test circuit using a small scale model. It extracts the transformer and the ShR from Fig. 3.

In terms of analysis, a current zero-missing occurs in the grid connection CB when current with a DC component flows from the ShR to the fault point. However, given that

a transformer is designed to supply current from the primary side to the secondary side by electromagnetic induction, constant DC with no AC component cannot pass due to the working principle. Here, if current with a DC component generated by the ShR does not flow to the grid connection CB side due to transformer action, it is unnecessary to implement measures against short-circuit current zero-missing. Thus, we conducted an evaluation using a small-scale model based on actual measurement and studied the need to implement countermeasures.

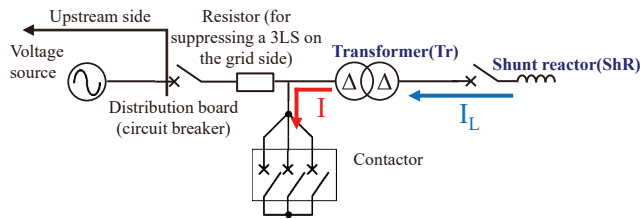


Fig. 9. Test circuit for short-circuit current zero-missing phenomenon

(1) Configuration of the verification equipment

Table 3 shows the circuit parameters of the equipment used for the test. The transformer is designed to flexibly change the connection for various types of studies.

Table 3. Circuit parameters

Equipment	Item		
	Connection	Δ - Δ	
Three-phase transformer 100 V / 100 V	Capacity	1.75	kVA
	Winding resistance (primary + secondary) R	103	m Ω
	Leakage inductance L	0.296	mH
	Winding resistance R	125	m Ω
Shunt reactor (ShR)	Inductance L	14.6	mH

(2) Test results

The test results are shown in Fig. 10 as current voltage waveforms. Current with a DC component starts to flow from the ShR at $t = 0$ ms, when voltage reaches zero due to a 3LS. The figure shows that similar current flows on the CB current side. This is not constant DC and is attributed to changes in the magnetic flux in the transformer. Accordingly, even if a transformer is present, current with a DC component flows from the ShR. A current zero-missing is likely to occur depending on the timing of a fault.

The decay time constant τ can be calculated as indicated below based on the actual measurement values of R and L.

$$\tau = L/R = (14.6 + 0.296)/(125 + 103) = 65 \text{ ms}$$

The CB current at fault inception ($t = 0$ ms) is 8.8 Ap. The waveform shows that the timing when the amplitude reaches 36.8% (3.2 Ap) based on the definition of time

constant is 70 ms. The error is approximately 10%. Thus, the test results are appropriate, and the decay time constant can be calculated accurately.

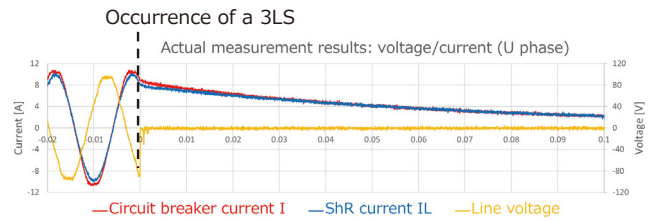


Fig. 10. Test results (waveform) of a short-circuit current zero-missing phenomenon

5-2 Magnetizing inrush current test: flux contribution from the Δ winding

For Y- Δ connected transformers, the capacity of the stabilizing winding must be determined by taking into account the fact that a current 1/2-fold that of magnetizing inrush current also flows on the Δ connection side due to flux contribution when the iron core on the Y connection side is saturated and magnetizing inrush current is generated. This section presents the results of the evaluation of flux contribution from the Δ winding, which is one of phenomena related to magnetizing inrush current, using a small-scale model.

When a three-phase transformer is energized with zero voltage on the U phase, magnetizing inrush current of other phases is considered to be smaller than that of the U phase because of a 120-degree phase difference. Here, when voltage is applied from the Y connection side in an ungrounded neutral point system and the iron core is saturated only on the U phase, the magnetizing inrush current path is as shown in Fig. 11.

On the assumption that magnetizing current on the U phase is I , magnetizing inrush current on the U phase that flows from the grid is $2/3 \cdot I$, and the current is equally divided into the V phase and W phase. However, these two phases do not require magnetizing current, such as inrush current, because they are not magnetically saturated. Thus,

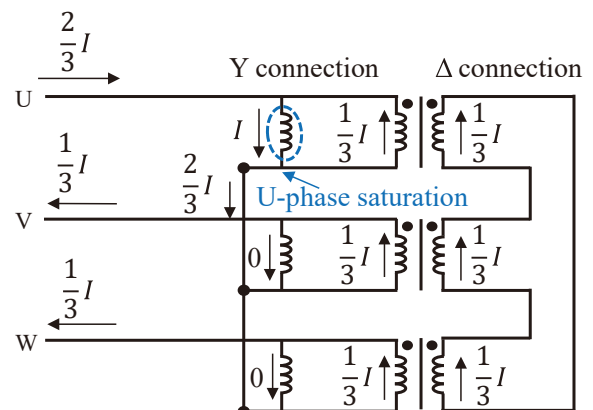


Fig. 11. Diagram illustrating flux contribution from the Δ winding

current that offsets the ampere-turns attributed to the $1/3 \cdot I$ current flows through the Δ winding, which is a non-energized winding, on the V phase and W phase.

The current in the Δ winding circulates and also flows to the U phase, which generates magnetizing inrush current, supplying ampere-turns from the Δ winding. On the U phase, the sum of the current circulating in the Δ winding ($1/3 \cdot I$) and the current flowing from the line ($2/3 \cdot I$) should be the magnetizing current ($= I$ in Fig. 11). Thus, the U-phase magnetizing inrush current that flows into the Y winding is $2/3 \cdot I$.

That is, when the Y winding of a Y- Δ connected three-phase transformer is energized from a three-phase power source, if magnetizing inrush current is generated on one phase only, the magnitude of the magnetizing inrush current that flows to the line of the phase is 2/3-fold that of the magnetizing current. This phenomenon is referred to as the flux contribution of the Δ winding.⁽⁶⁾

A small-scale model was used to measure the magnetic flux and current of each phase and the Δ winding current when the three phases are energized.

(1) Configuration of the verification equipment

The test circuit diagram is shown in Fig. 12. The same transformer for the test described in Section 5-1 is used. The connection is changed to Y- Δ . The CB is closed when the U-phase magnetic flux reaches its maximum ($V_u = 0$ V).

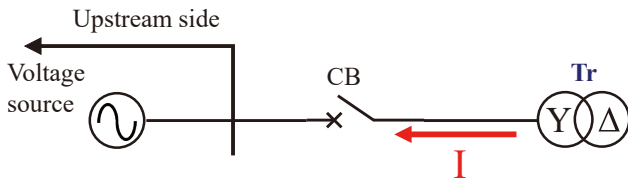


Fig. 12. Circuit diagram for magnetizing inrush current testing

(2) Test results

Figure 13 shows the test results, which are represented by magnetic fluxes (integral of the voltage) and current waveforms. For example, the dashed line of the U saturation peak shows that the line current of other phases is approximately 1/2-fold that of the line current of the saturated phase. It can also be confirmed that a current offsetting the ampere-turns of the unsaturated phase flows through the Δ winding. It should be noted that the three phases are energized at the same time in this test. Thus, when one phase is saturated, the other phases also become saturated. Accordingly, V-phase and W-phase currents represent the total value of saturated current and current in the Δ winding. Current in the Δ winding does not match the phase currents, and this is different from the explanation about the working principle discussed above. Similar waveforms are observed in the saturated regions in the V and W phases.

The evaluation results derived from the test are valuable in that actual flux contribution has been verified because the structure of ordinary transformers hinders evaluation of the current in the Δ connection.

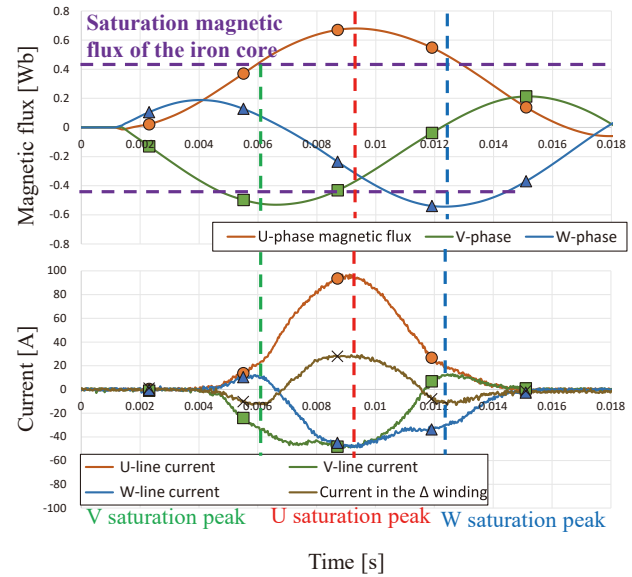


Fig. 13. Test results (waveform) of magnetizing inrush current

6. Conclusion

This paper explained how our grid analysis technologies contribute to stable operation of WFs during grid connection based on examples of studying abnormal phenomena during grid connection via long-distance cables and conducting preliminary evaluations for stable system operation. The grid characteristics are expected to become more complex due to an additional increase in WFs, and cable lengths are expected to be extended for grid connection of large-scale offshore WFs. We will continue to harness our grid analysis technologies to identify issues in WF systems, study operational measures, and thereby contribute to the expansion of WFs.

References

- (1) Agency for Natural Resources and Energy, "Overview of the Energy Basic Plan," p. 9 (2025)
- (2) Agency for Natural Resources and Energy, "Future Renewable Energy Policies," p. 21 (2025)
- (3) K. Ota, S. Mayama, and M. Tanaka, "Design Methods of Power Cable Transmission Systems for Large-Scale Installation of Renewable Energy," SUMITOMO ELECTRIC TECHNICAL REVIEW No. 93 (October 2021)
- (4) Y. Tanaka, H. Uemura, N. Nagasaki, K. Kuroda, Y. Ogihara, S. Mayama, and K. Ohta, "Possible Harmonic Resonance Problems and Mitigation Proposals -Preparing for the age of renewable energy resources as major power generation-, " SUMITOMO ELECTRIC TECHNICAL REVIEW No. 203 (July 2023)
- (5) "Cooperation between Power Equipment and System Protection," IEEJ Technical Report, no. 898, pp. 114-117
- (6) "Cooperation between Power Equipment and System Protection," IEEJ Technical Report, no. 898, pp. 77-78

Contributors The lead author is indicated by an asterisk (*).

K. HAMASAKI*

• Nissin-Sumiden Energy System R&D Center

**T. IIMURA**

• Nissin-Sumiden Energy System R&D Center

**K. KURODA**

• General Manager, Nissin-Sumiden Energy System R&D Center

**T. ADACHI**

• Director, Nissin Electric Co., Ltd

**N. NAGASAKI**

• Special fellow, General Manager, Nissin Electric Co., Ltd

**H. UEMURA**

• Senior Adviser, Nissin Electric Co., Ltd

